BUTTERWORTH HEINEMANN

Polymer Vol. 36 No. 26. pp. 4951–4960, 1995

0032-3861/95/$10.00+0.00

Kinetics of droplet growth in liquid–liquid phase separation of polymer–diluent systems: experimental results

Kenneth S. McGuire, Anand Laxminarayan and Douglas R. Lloyd*
Center for Polymer Research, Department of Chemical Engineering, The University of Texas at Austin, Austin, TX 78712, USA
(Received 4 January 1995)

Liquid–liquid thermally induced phase separation of the polymer–diluent system isotactic poly(propylene)–diphenyl ether was studied under an optical microscope. It was found that as the system phase separated, droplets of a diluent-rich phase formed within a polymer-rich matrix. These droplets grew in size and decreased in number by a process known as coarsening. The scaling exponent relating droplet diameter and time was determined. The scaling exponent was found to be a strong function of the droplet phase volume fraction, and this strong dependence on volume fraction was relatively insensitive to temperature. The influence of the ratio of interfacial tension between the phases and the viscosity of the matrix phase was less significant on the growth rate of the droplets.

(Keywords: droplet growth; liquid–liquid phase separation; polymer–diluent systems)

INTRODUCTION

When a polymer–diluent solution is cooled from the homogeneous one-phase region of the phase diagram to a temperature within the coexistence curve, liquid–liquid thermally induced phase separation (TIPS) occurs. In many systems, droplets of one phase form within a continuous matrix of a second phase. These two phases have compositions given by the coexistence curve. In the formation of cellular membranes via TIPS, the droplet phase is diluent-rich and the matrix phase is polymer-rich. Through a process known as coarsening, these droplets grow with time once they have reached their equilibrium compositions. The thermodynamic driving force for this droplet growth is the minimization of interfacial free energy via reduction of the interfacial area. Thus, for a system with a constant volume fraction of droplets, the droplets increase in size and decrease in number with time. When the polymer is solidified by a drop in temperature and the diluent is removed, the droplets become the cells in the membrane. The size of the droplets at any instant in time in a phase-separated system is a direct reflection of the size of the cells in the resulting membrane if the polymer were solidified and the diluent removed. Therefore, the objective of this study was to measure experimentally the droplet size as a function of the independent variables temperature, initial polymer concentration and time for the model system isotactic poly(propylene)–diphenyl ether. The equilibrium phase diagram reported elsewhere[1] was used to determine the conditions under which liquid–liquid TIPS occurs.

* To whom correspondence should be addressed

BACKGROUND

Most of the studies on polymer–diluent systems have been morphological in nature[2–9]. Membranes in these studies were generally made from glassy polymers such as poly(methyl methacrylate)[2–4] and polystyrene[5–9]. Other detailed studies of the coarsening phenomena generally entail measuring the domain size, r, as a function of time, t, and expressing this growth rate with a scaling relationship,

$$r \propto t^{\lambda} \tag{1}$$

where λ will hereafter be referred to as the scaling or growth exponent. The domain size has been monitored by electron microscopy[9,10], light scattering[11–13], and optical microscopy[14,15]. In these studies, the scaling exponent was normally determined for several temperatures and polymer concentrations within the coexistence curve. Currently available models predict a constant scaling exponent for each mechanism of domain growth—an exponent of $\frac{1}{3}$ for both the coalescence and Ostwald ripening models and an exponent of 1 for the filament growth model[16]. However, for the studies for polymer–diluent systems, it has been observed that the scaling exponent is a function of the quench condition. For example, Nojima *et al.*[15] report scaling exponents ranging from 0.208 to 0.392 as polymer concentration and temperature of the quench are varied. The interested reader is referred to ref. 17 for a detailed review of the scaling exponents reported by previous researchers in polymer–diluent systems. A unified theory describing discrepancies between experimental observations and the currently available growth models is lacking in the literature.

Previous kinetic studies for polymer–diluent systems undergoing liquid–liquid TIPS

Smolders and co-workers were the first research group to publish the results of a kinetic study for a polymer–diluent system undergoing liquid–liquid TIPS[18]. They used a poly(2,6-dimethyl-1,4-phenylene ether) (PPO)–caprolactam system. In this study, it was observed under an optical microscope that droplets of a polymer-rich phase were formed within a polymer-lean matrix. They report that these drops increased in size with time. In particular, they note that as the quench temperature decreased, the droplet growth rate increased. Further, as the initial polymer concentration increased, the droplet growth rate increased. Not only was this the first reported kinetic study for a polymer–diluent system undergoing liquid–liquid TIPS, it was also the first to show a discrepancy between experimental observations and existing theories: none of the theories described in the preceding section predict a change in the scaling exponent as the temperature or initial solution concentration changes. Smolders attributed this behaviour to a process that was later to be termed coarsening—the process by which the system's interfacial free energy is minimized once the phases have reached their equilibrium concentrations.

Some 11 years after the study by Smolders *et al.*, a more detailed study on the kinetics of droplet growth in liquid–liquid TIPS for a polymer–diluent system was published by Nojima and co-workers[15]. The system that was used in this study was nearly monodisperse molecular weight polystyrene in diisodecyl phthalate. The droplet growth was monitored under an optical microscope. In this study, droplets of the polymer-lean phase formed and grew in a polymer-rich matrix phase, which contrasts with the system studied by Smolders[18], as described in the previous paragraph. Nojima reported the growth rate data using the scaling exponent described in the previous section. He found that the scaling exponent increased as the temperature decreased and as the initial polymer concentration decreased. The scaling exponents in this work ranged from 0.208 to 0.392. The authors attributed the droplet growth to Ostwald ripening or coalescence (no distinction between the two can be made based only on the magnitude of the exponent), and attributed the deviation from the theoretically predicted exponent of $\frac{1}{3}$ to experimental error. However, in this study, the magnitude of error in the exponents was not reported, and no reproducibility measurements were performed. Based on the microscope studies, Nojima *et al.* further argued that the volume fraction of droplets remained constant after a certain induction or nucleation time (typically about 400 min for this system), but these results seem somewhat inconclusive due to the large amount of scatter in the data.

The research group of Bansil and co-workers has published two kinetic studies on liquid–liquid TIPS for polymer–diluent systems[13,14]. A nearly monodisperse molecular weight polystyrene–cyclohexane system was used in both studies. In the first study, phase separation was monitored under an optical microscope using a 35 mm camera to record the phase separation for subsequent analysis[14]. This study was relatively short, and utilized only two different polymer concentrations, both quenched to the same degree of undercooling beneath the coexistence curve. One sample produced polymer-lean droplets in a polymer-rich matrix, and the other produced polymer-rich droplets in a polymer-lean matrix. Although scaling exponents were not reported by the authors of the study, they have been calculated by the present authors from the reported data. An exponent of 0.03 was calculated for the polymer-rich droplets and an exponent of 0.53 was calculated for the polymer-lean droplets. Bansil attributes any deviations from the Ostwald ripening theory to gravity-induced coalescence, but no effort was made to model this type of mechanism mathematically.

In the second and more complete study by the Bansil research group, phase separation was monitored by light scattering[13]. Two different molecular weights of polystyrene were used in this study, varying by a factor of ten. The diluent used was cyclohexane. Scaling exponents were reported for a variety of quench temperatures for each polymer, and they varied from 0.43 to 0.59. No systematic variation with temperature was observed for either sample. The authors attribute the deviation from the theoretically predicted Ostwald ripening exponent of $\frac{1}{3}$ to hydrodynamic effects. Unfortunately, not only do the authors fail to mention whether droplets exist in the system (or if it is a lacy structure), or if the droplets are polymer-lean or polymer-rich, but there is no analysis of the experimental error. Any systematic changes in the scaling parameter could be masked by unreported experimental error. This study points out one of the weaknesses in using light scattering to measure the kinetics of phase separation: since the phase separation of the system is not visually observed, the morphology of the phase-separating system, and thus the possible coarsening mechanism, cannot be as easily identified as with direct microscopic observation.

The liquid–liquid TIPS research of Aubert has also focused on the polystyrene–cyclohexane system. In a recently published study, the 'spacing' between polymer strands in a membrane formed via liquid–liquid TIPS was measured as a function of time[19]. Aubert used the term 'spacing' as opposed to diameter, because SEM photomicrographs of these membranes revealed a lacy polymer structure as opposed to a cellular structure—apparently droplets were not formed in this system. Aubert used a unique method to measure this spacing. The internal surface area of a given section of the membrane was measured using a gas adsorption method, and this area was related to the spacing using stereology. Aubert found scaling exponents ranging from 0.18 to 0.32, but stated that scatter in the data prevented statistical differentiation between these exponents. To explain the growth rate, Aubert developed a model known as 'diffusive coarsening' which was based on the same phenomenon as the Ostwald ripening mechanism, but could be applied to highly interconnected systems. His new model predicted a scaling exponent of $\frac{1}{3}$ irrespective of the quench temperature or solution concentration. One drawback of using the gas adsorption method for determining spacings is that the solution must be solidified (in this case by vitrification of the polymer-rich phase), and the diluent must be extracted from the system. These processing steps may affect the morphology and the dimensions of the resulting membrane structure and make it difficult to relate the final membrane morphology to the original phase-separating system.

Table 1 Kinetic studies of liquid–liquid phase separation in polymer–diluent systems

Researchers	System	Method[a]	λ
Smolders and co-workers[18]	Polyphenylene ether–caprolactam	OM	No data
	Ethylene–vinyl acetate copolymer–caprolactam		
Nose and co-workers[15]	Polystyrene–diisodecyl phthalate	OM	0.208–0.392
Laxminarayan[11]	Polystyrene–cyclohexanol	SEM	0.60
Aubert[5–7]	Polystyrene–cyclohexane	BET	0.18–0.36
		SEM	
Lal and Bansil[13]	Polystyrene–cyclohexane	LS	0.4–0.5
Song and Torkelson[10]	Polystyrene–cyclohexanol	SEM	0.05–0.9
	Polystyrene–cyclohexane polystyrene–diethyl malonate	MIP	

[a] OM, Optical microscope; SEM, scanning electron microscope; LS, light scattering; MIP, mercury intrusion porosimetry; BET, Brunauer–Emmett–Teller method of measuring surface area

Torkelson has recently published a study of coarsening for two polymer–diluent systems: polystyrene–diethyl malonate and polystyrene–cyclohexane. The polystyrene–diethyl malonate system is stated in this work to be isopycnic—that is, the polymer and diluent have nearly the same densities so that gravitational effects during coarsening may be ignored. It is not reported whether the phases formed upon phase separation have the same densities. Cell sizes in this study were measured by SEM and by mercury porosimetry, and fair agreement was found between the two methods: the majority of the droplet sizes were determined by SEM. Unfortunately, since the experiments were not monitored under an optical microscope, it is unclear whether the cell sizes measured after the diluent was removed are equal to the droplet sizes formed during phase separation. For the polystyrene-diethyl malonate system, it was found that initially the scaling exponents ranged from 0.08 to 0.33 and increased with decreasing temperature. However, if the system was allowed to phase separate for extremely long periods of time—greater than 1000 min—the scaling exponent asymptotically approached 1. It is not reported whether the phases formed upon phase separation have the same densities. No explanation was given for the range of exponents between 0.08 and 0.33 at early times. For the polystyrene–cyclohexane system, scaling exponents ranged from 0.05 to 0.30, and no transition toward an exponent of 1 was seen at long times.

Table 1 summarizes scaling exponents reported in the literature along with the systems studied and the method of experimentally determining the exponent.

MATERIALS AND METHODS

Materials

Commercially, it is of great interest to produce membranes from polymers that can withstand high operating temperatures and harsh chemical environments present in some applications. Because semi-crystalline polymers show superior thermal and chemical resistance when compared to their amorphous counterparts, it was of interest to make membranes in this study from a semi-crystalline polymer. Isotactic poly(propylene) (iPP; Fina lot No. 20769; $M_w = 168\,000$) was chosen as the candidate polymer for this reason and for others.

1 It is currently being used commercially to make microporous polymeric membranes[20–22].
2 Its properties are well documented in the literature[23,24].

The diluent chosen for this study was diphenyl ether (DPE; Aldrich Chemicals; 99% purity). It was chosen for the following reasons.

1 It has a high normal boiling point (532 K), which minimized diluent evaporation during membrane formation.
2 It has a low molecular weight (170 g mol^{-1}), which allowed for relatively quick extraction.
3 It has a significantly different refractive index from iPP, which allowed the liquid–liquid phase separation to be viewed under an optical microscope.
4 It exhibits a relatively large miscibility gap with iPP[25], which allowed the kinetics of droplet growth to be measured at a variety of temperatures and compositions.

Since DPE is miscible at high concentrations with methanol, and because methanol does not swell iPP to any appreciable extent, methanol (Sigma Chemicals; 99+% purity) was chosen as the extractant.

It was desired to study the kinetics of droplet growth at a variety of temperatures and mixture compositions within the liquid–liquid phase separation region. The determination of the phase diagram for the model system is reported elsewhere[1] and is shown here as *Figure 1*. If the polymer crystallizes during liquid–liquid TIPS, droplet growth may be hindered or halted altogether[26]. Thus, the experiments had to be carried out inside the coexistence curve to ensure liquid–liquid TIPS and at temperatures high enough to prevent polymer crystallization. In the light of these restrictions, it was decided

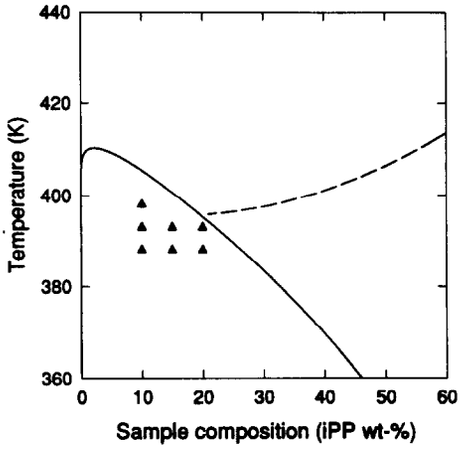

Figure 1 Phase diagram of the iPP–DPE system. — Coexistence curve; – – – melting-point depression curve; ▲, conditions at which droplet growth experiments were carried out

Table 2 Conditions under which droplet growth rate experiments were carried out

Temperature (K)	Composition (iPP wt%)		
	10	15	20
398	X		
393	X	X	X
388	X	X	X

Table 3 Polymer-rich phase compositions at the temperatures at which droplet growth experiments were conducted

Temperature (K)	Polymer-rich phase composition	
	Wt% iPP	Vol% iPP
398	17.5	21.1
393	22.5	26.8
388	26.5	31.3

that the droplet growth experiments would be carried out at the temperatures and compositions listed in *Table 2* and shown graphically in *Figure 1*. Compositions of the polymer-rich phase at the three temperatures of interest were determined from the phase diagram and are reported in *Table 3*. In converting from wt% to vol% it was assumed that no volume change occurred on mixing.

The lowest polymer concentration to be studied was 10 wt% iPP. This lower bound was determined by the polymer–diluent sample-making procedure described below. It was not possible using this procedure to make reproducible, homogeneous polymer–diluent samples with polymer concentrations less than 10 wt%. Also, the viscosities of the resulting melted samples with concentrations less than 10 wt% were so low that they tended to 'run out' from between the glass slides during optical microscopy experiments.

The lowest temperature at which extensive droplet growth experiments were carried out was 388 K. This lower bound on temperature was determined by polymer crystallization. It can be seen in *Figure 1* that the experiments carried out at 393 and 388 K were below the melting point depression curve, and thus there was a thermodynamic driving force for polymer crystallization at these temperatures. However, during the time-scale of the experiments (typically 10 min) no polymer crystallization was observed. Polymer crystallization was observed under the optical microscope at 388 K after approximately 45 min.

Sample preparation for kinetic studies

Homogeneous polymer–diluent samples were prepared in a test tube. The desired amounts of polymer and diluent were weighed into a 13 mm × 100 mm borosilicate test-tube to a total sample mass of 2 g. The test-tube was purged with nitrogen for 20 min and then flame sealed using a propane–oxygen flame. The test-tube was then placed in a convection oven at 473 K for 24–48 h, removed from the oven, and quenched in liquid nitrogen. When broken open, the test-tube yielded a solid, cylindrical homogeneous polymer–diluent sample.

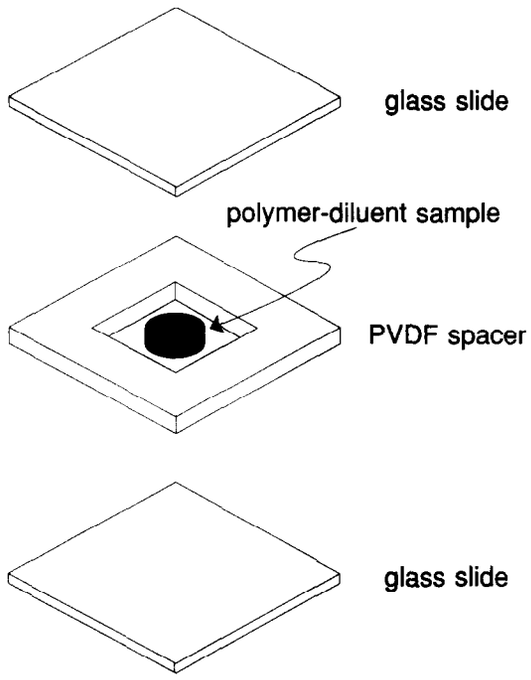

Figure 2 Exploded isometric view of the apparatus used to hold the polymer–diluent sample for the droplet growth experiments

Extraction studies have been done to test the homogeneity of the resulting samples, and it has been shown that at various locations throughout the sample, the polymer concentration varied by less than ±2 wt% polymer[27].

For the optical microscopy studies, a small amount of the polymer–diluent sample was sandwiched between two glass microscope coverslips separated by a 50 μm thick poly(vinylidene fluoride) (PVDF) spacer (*Figure 2*). The PVDF spacer was used for two reasons:

1 The uniform thickness of the spacer allowed samples of uniform thickness to be prepared for the optical microscopy studies from one sample to the next.
2 The spacer limited diluent evaporation during the course of the experiment.

Droplet growth kinetic studies

A hot stage (Linkham HFS-91) was placed on the platform of an optical microscope (Nikon Optiphot2-Pol). The hot stage was controlled with a Linkam TMS-91 controller and a Linkam CS-196 cooling unit. The image from the optical microscope was converted to a video signal with a digital camera and controller (COHU 6500). The video signal was passed through a FOR.A video timer and into a *S*-VHS videocassette recorder (Panasonic AG-1960) where it was captured on a *S*-VHS videotape (3M ST-120) for subsequent analysis. The image was simultaneously broadcast to a video screen, where the video image was monitored. Still photos from the videotape were taken with a Polaroid Freeze Frame Video Recorder.

The optical microscope was fitted with a long focal length, 30× Hoffman Modulation Contrast objective lens. The long focal length lens was used because of the depth of the hot stage. This objective lens resulted in a field of view on the video screen of 200 μm × 150 μm.

To measure the droplet size at any time, digital image analysis was used. The image was captured from the videocassette with an 8-bit black and white framegrabber (ITI-OFG) mounted in a 486-33 personal computer. The image analysis software package used was Bioscan OPTIMAS. The image was displayed on a black and white video monitor (Sony PVM-122) during image analysis. Based on the objective lens used on the optical microscope and the resolution of the frame grabber, the smallest droplet diameter that could be measured was approximately 2 μm. Droplets smaller than 2 μm occupied such a small number of pixels on the digitized image that they appeared square.

Interfacial tension

Owing to experimental difficulties[16], the interfacial tension was estimated from the surface tensions (the surface tension of a phase is the interfacial tension between that phase and air) of the two coexisting phases using the Fowke's relationship[28],

$$\gamma_{12} = (\gamma_1^{1/2} - \gamma_2^{1/2})^2 \quad (2)$$

where γ_{12} is the interfacial tension, γ_1 is the surface tension of the polymer-rich phase, and γ_2 is the surface tension of the polymer-lean phase. The surface tensions of the two phases were measured in a spinning drop tensiometer[29]. In the tensiometer, an air bubble was introduced into a homogeneous mixture in a capillary, and the bubble diameter was measured as a function of the rate at which the capillary was spinning. Measurements were made at the three temperatures and compositions listed in *Table 3*. It was assumed for these measurements that the polymer-lean phase was 100% diphenyl ether. Details of the measurements were given elsewhere[16].

Viscosity of polymer-rich phase

The viscosity of the polymer-rich phase at the three temperatures of interest and compositions listed in *Table 3* were measured in a Fann 50C cup and bob viscometer. Details of the measurement technique are given elsewhere[30].

Scanning electron micrographs

Scanning electron micrographs (SEMs) of membranes made by TIPS were obtained as follows. A sample similar to those used for cloud point measurements was removed from the hot-stage following the appropriate thermal treatment. The sample was immersed in liquid nitrogen to freeze the structure. After removing the sample from between the glass slides, the diphenyl ether was extracted with methanol (Sigma, spectrophotometric grade) for 24 h, and the resulting microporous structure was dried under vacuum overnight at room temperature. After the membrane was removed from the vacuum oven, it was fractured in liquid nitrogen and coated with 5–12 nm of gold–palladium using a sputtering coater (Commonwealth Model 3, Pelco). The cross-section of the membrane was photographed on a Jeol JSN-35C microscope under an accelerating voltage of 25 kV.

RESULTS AND DISCUSSION

Interfacial tension

The measured surface tensions are reported in *Table 4*, as are the corresponding interfacial tensions.

Viscosity

The viscosities of the polymer-rich phases were measured at a variety of shear rates ranging from 4 to 20 s^{-1}, and it was found that the viscosities were not strongly dependent on shear rate[30]. The measured viscosities at the three temperatures and compositions of interest are reported in *Table 5* at a shear rate of 17 s^{-1}.

Droplet phase volume fraction

The droplet phase volume fraction is a crucial parameter in any kinetics model used to describe the growth of droplets in a liquid–liquid TIPS process. In this work, the droplet phase volume fraction was determined from the phase diagram shown in *Figure 1*.

Kinetic droplet growth data was taken at seven experimental conditions, corresponding to seven potentially different droplet phase volume fractions. The lever rule was used to compute the volume fraction of the droplet phase at all seven experimental conditions[31]. The values for the droplet phase volume fractions are listed in *Table 6* for each of the seven experimental conditions.

Table 4 Measured surface tensions and calculated interfacial tensions for isotactic poly(propylene)–diphenyl ether. Relative error is listed in the table

	Surface and interfacial tensions (dyne cm^{-1})		
Temperature (K)	γ_1	γ_2	γ_{12}
398	16.64 ± 0.42	14.60 ± 0.37	0.067 ± 0.036
393	19.90 ± 0.50	15.59 ± 0.39	0.242 ± 0.077
388	21.95 ± 0.55	16.60 ± 0.42	0.373 ± 0.095

Table 5 Viscosities of the polymer-rich phases. Error in the measurement was determined elsewhere[30]

Sample composition, temperature (polymer wt%, K)	Viscosity, η (poise)
17.5, 398	14.1 ± 2.3
22.5, 393	119 ± 19
26.5, 388	207 ± 19

Table 6 Droplet phase volume fractions for each of the seven experimental conditions used in the droplet growth studies

	Initial sample composition (iPP wt%)		
Temperature (K)	10	15	20
398	0.42	–	–
393	0.54	0.32	0.10
388	0.61	0.42	0.23

Droplet growth kinetics

The sample on the hot stage was heated at 100 K min^{-1} from room temperature to 433 K (in the one phase region in *Figure 1*) where it was held for 5 min. The 5 min holding time was chosen to allow the sample to homogenize, to remove thermal history, and to limit diluent evaporation. The temperature was then dropped at 130 K min^{-1} (the maximum controlled cooling rate of the hot stage) to the phase separation temperature of interest. In this work, time $t = 0$ was defined as the time at which the sample reached the phase separation temperature.

As the temperature of the polymer–diluent sample was dropped from 433 K to the phase separation temperature at 130 K min^{-1}, an interconnected structure initially developed. It has sometimes been claimed in the literature that this interconnected structure is indicative of spinodal decomposition[3,5]. However, it has also been shown that the appearance of an interconnected structure is not proof of the spinodal decomposition mechanism[32]. No attempt has been made in this study to differentiate between spinodal decomposition and nucleation and growth as the initial phase separation mechanism. The appearance of the interconnected structure is simply reported here as an experimental observation. It was further observed, at all conditions, that the interconnected structure broke up into droplets that grew in time and decreased in number (*Figure 3*). Others have observed interconnected structures breaking up into droplets in liquid–liquid TIPS for polymer–diluent systems[3,33]. The sizes of the cells that result from diluent removal correspond to the size of the droplets formed during phase separation (*Figure 4*).

As described in the introduction to this paper, it was of interest in this study to determine the growth rate of these drops as a function of phase separation temperature and initial polymer concentration. In this system, as in others, a distribution of droplet sizes exists at every instant in time. Therefore, prior to reporting the results of the kinetic studies, typical droplet size distributions are reported. Further, a check on the reproducibility of the method of measuring droplet sizes is presented.

Droplet size distributions

To determine an accurate and statistically meaningful droplet size distribution, a large number of drops must be measured. However, this was not always possible due to the optical 'overlap' of many of the drops viewed under the optical microscope. One experimental condition was chosen that had fairly good resolution of a larger number of droplets; the image taken from the optical microscope at this condition (*Figure 5*) shows a large number of round drops. To measure the diameters of these drops, the following procedure was used.

1 A drop was randomly selected for measurement, and its circumference was traced manually in the image analysis program.

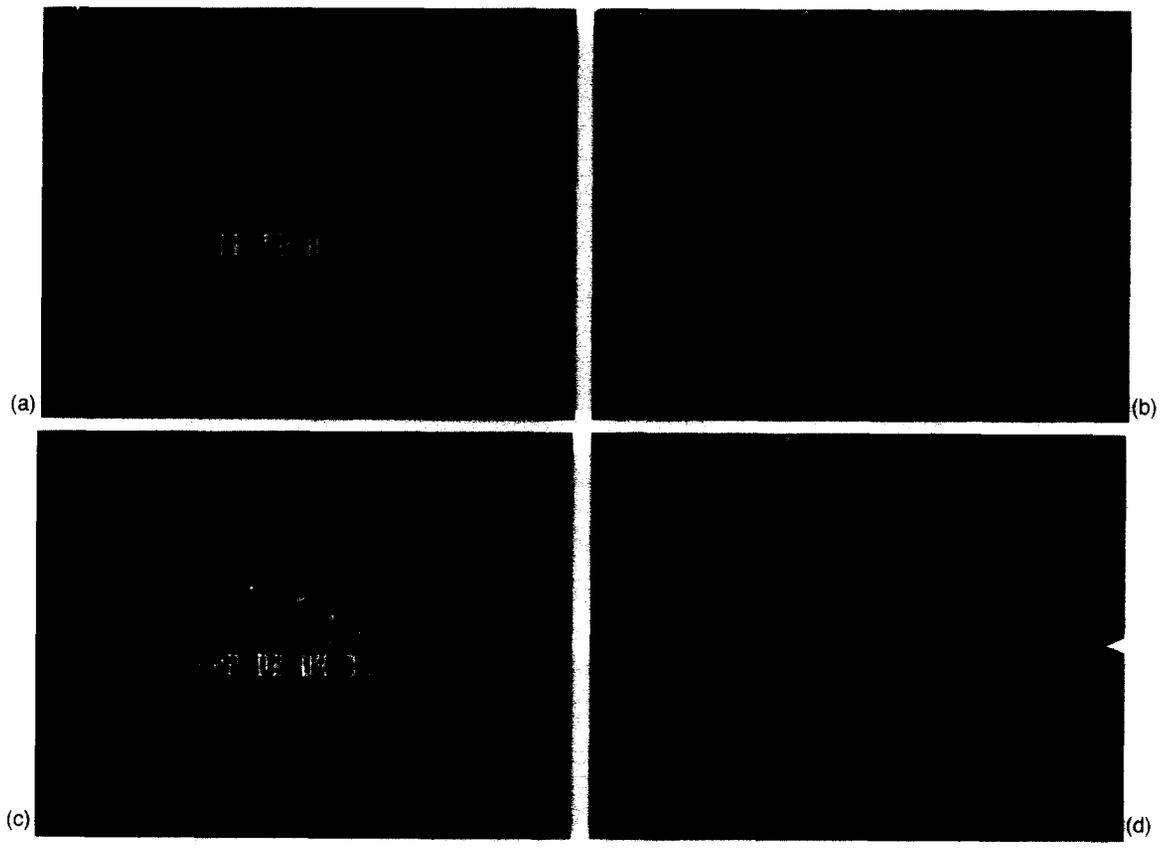

Figure 3 Optical micrographs of droplets formed from a 20 wt% iPP sample phase separating at 388 K for (a) $t = 60$ s, (b) $t = 120$ s, (c) $t = 250$ s, (d) $t = 500$ s

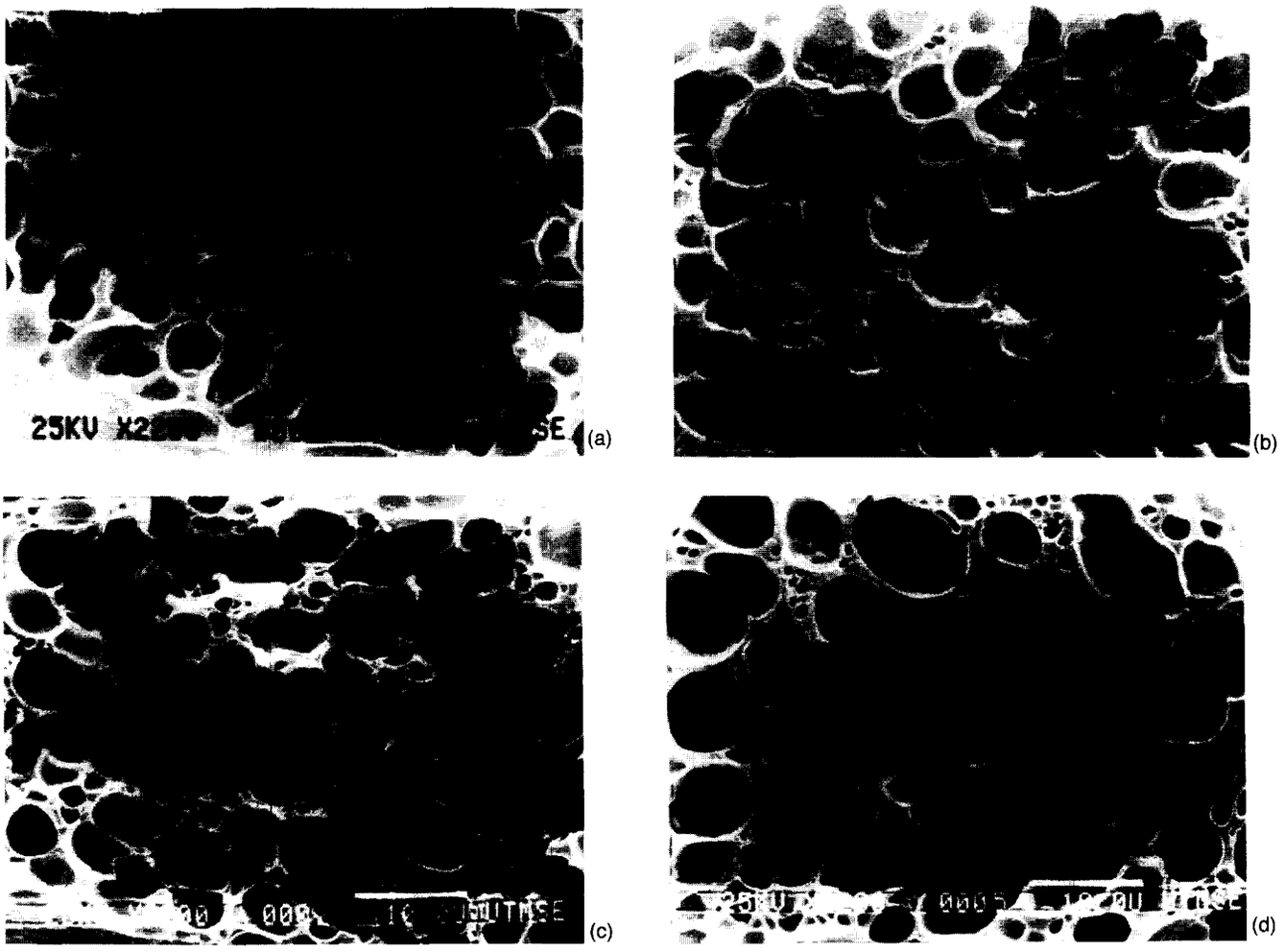

Figure 4 SEM cross-sections of membranes made from a 20 wt% iPP sample phase separated at 388 K for (a) $t = 60$ s, (b) $t = 120$ s, (c) $t = 250$ s, (d) $t = 500$ s

2 After a suitable number of drops had been marked in this manner (47 were selected and traced for the distribution measurement), their cross-sectional areas were computed by the image analysis program.

Figure 5 Optical micrograph used for droplet size distribution determination of a 15 wt% iPP sample phase separated at 393 K for 337 s

3 The droplet areas were converted to diameters by assuming that the drop cross-sections were circular.

Figure 6 shows the histogram that resulted from measuring 47 droplet diameters (the maximum number of measurable drops) in *Figure 5* by the method outlined above. The mean droplet diameter was determined from the 47 measured diameters to be 17.03 μm and the standard deviation was determined to be 3.46 μm. The distribution is quite broad with the smallest measured diameter being 8.23 μm and the largest being 24.30 μm. The dotted reference curve in *Figure 6* is a Gaussian distribution with the same mean and standard deviation as the histogram.

Reproducibility of droplet measurements

In determining the droplet growth rates, the average droplet size was used. Typically, between 20 and 25 droplets could be measured at each frame of time using the same method described in the previous section for measuring drops. Although the entire system contains many thousands of drops, only 50–100 appear in the field of view at one time. Of these, only 20–25 have distinct enough edges to be measured with accuracy. To test the accuracy and reproducibility of measuring the 20 to 25 drops, the following procedure was used.

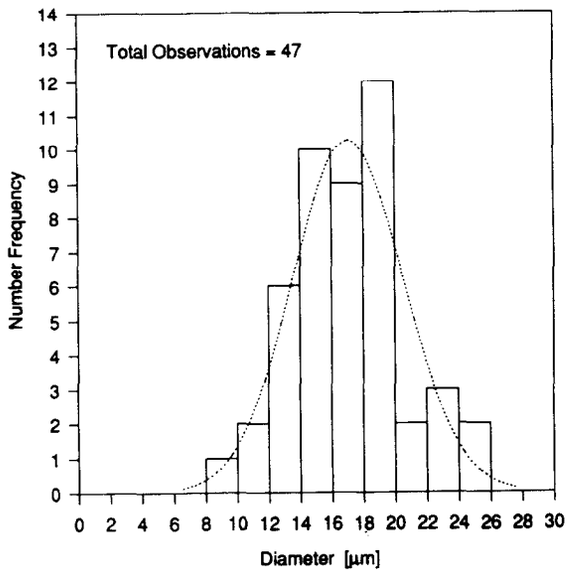

Figure 6 Histogram of droplet sizes determined from the optical micrograph shown in *Figure 5*. Dotted line is a Gaussian distribution fit to the histogram

1 The image shown in *Figure 5* was retrieved into the image analysis program.
2 Between 20 and 25 droplets were randomly selected.
3 The diameters were measured as described above.
4 The average diameter was calculated from the 20 to 25 measured diameters.
5 The image was cleared from the image analysis program.
6 This process was repeated until it had been completed ten times.

The average diameters ranged from 16.24 to 17.83 μm with the mean being 17.20 μm. The standard deviation of the ten independent measurements of the average diameters was found to be 0.58 μm (corresponding to 3.4% of the average). Therefore, the error in the reproducibility of measuring the droplet sizes was 3.4%. In all subsequent plots, the measurement error in each computed droplet diameter is assumed to be 3.4%.

Kinetic data

As described above, droplet growth rates were measured at the seven experimental conditions listed in *Table 2*. At each experimental condition, droplet growth experiments were carried out in triplicate with new polymer–diluent samples for each experiment. Typically, the average droplet diameter was measured at seven or eight different times for each experiment. Since each experiment was carried out in triplicate, this corresponded to approximately 20 data points for each experimental condition. The average diameter was determined by using the measurements of 20–25 randomly selected drops, as described in the previous sections.

Recall that time $t = 0$ was defined in this work to be the time at which the polymer–diluent sample reached the phase separation temperature. The sample was cooled at 130 K min^{-1} from 433 K to the phase separation temperature of interest so that all of the samples spent a small but finite amount of time inside the coexistence curve prior to $t = 0$. The amount of time that a sample spent within the coexistence curve prior to $t = 0$ increased with decreasing quench temperature and with decreasing initial polymer concentration. As soon as the temperature of a sample crosses the coexistence curve, phase separation is initiated and droplets begin to form. Thus, the size of droplets at time $t = 0$ varies depending on the quench condition.

Figures 7 to *9* show the kinetic data determined for each quench condition. Each plot contains data for a different quench temperature. Each set of data at a given temperature and composition represents three experiments. It is immediately apparent from examining the data that the quench condition has a strong influence on the rate of droplet growth. In general, as the quench

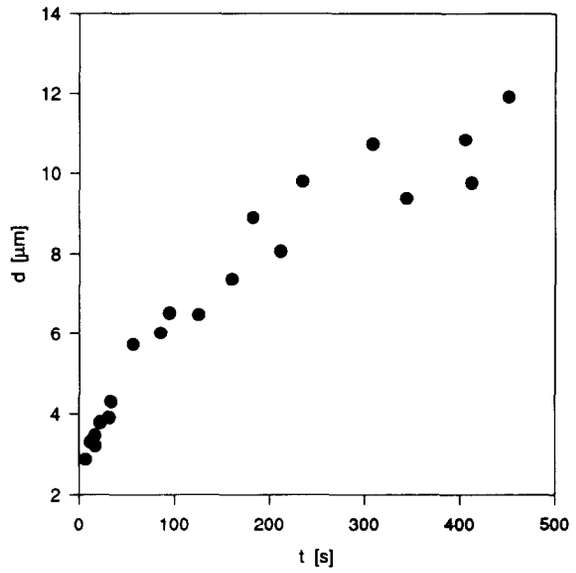

Figure 7 Average droplet diameter as a function of time for the 10 wt% iPP sample phase separated at 398 K

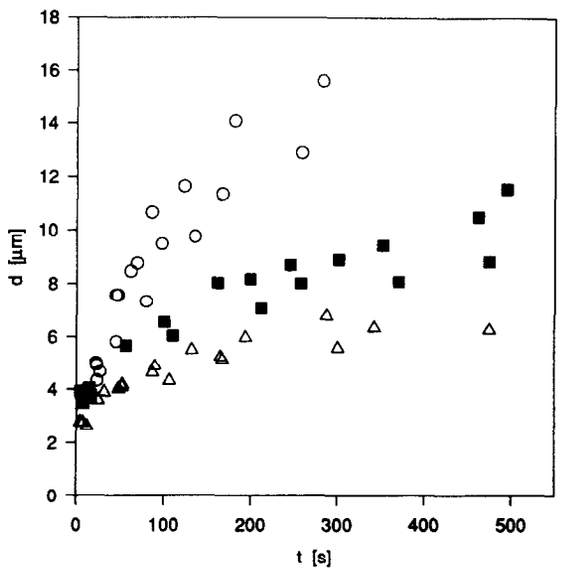

Figure 8 Average droplet diameter as a function of time at 393 K. ○, 10 wt% iPP; ■, 15 wt% iPP; △, 20 wt% iPP

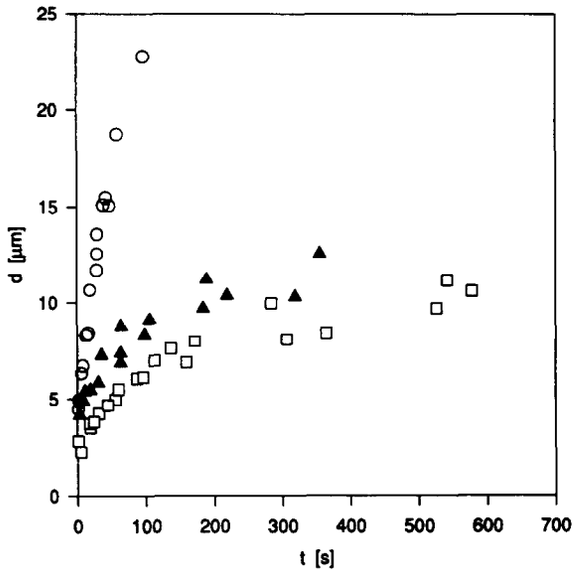

Figure 9 Average droplet diameter as a function of time at 388 K. ○, 10 wt% iPP; □, 15 wt% iPP; ▲, 20 wt% iPP

temperature decreases, or as the polymer concentration decreases, the growth rate increases. This same growth rate dependence has been observed by other researchers[10,15,19]. Of particular interest is the data of Smolders, which showed the same growth rate dependence on temperature, but the opposite dependence on polymer concentration. However, Smolders' system had polymer-rich drops growing in a polymer-lean matrix. This is just the opposite of the system studied in this work, which had polymer-lean drops growing in a polymer-rich matrix.

As described above, kinetic data for liquid–liquid TIPS experiments are usually reported by the scaling or growth rate exponent, λ (defined in equation (1)). In equation (1), r is a characteristic size (such as the droplet radius or diameter) and t is time. The exponent is the same regardless of whether the diameter or radius is used as the characteristic size. To determine the scaling exponent in this work, a log–log plot of droplet diameter against time was constructed and the slope of the curve was taken as λ. *Table 7* lists the experimentally determined growth rate exponents for each quench condition as well as their standard deviations.

It can be seen in *Table 7* that, in general, as the quench temperature is decreased, the scaling exponent increases. Further, as the polymer concentration in the sample increased, the scaling exponent decreased. These are the same trends observed in *Figures 7–9*, so the scaling exponent can be used as a quick reference to the growth rate of the droplets. In other words, as the growth rate increases, so does the scaling exponent. For the remainder of this work, the words 'growth rate' and 'scaling exponent' are used interchangeably. The 10 wt%, 393 K and the 10 wt%, 388 K exponents do not appear to follow the general trend mentioned in the first sentence of this paragraph; in fact, when the standard deviations are considered, these exponents are indistinguishable. To eliminate the possibility of error in determining the 393 and 388 K exponents, the 10 wt%, 388 K and the 10 wt%, 393 K experiments were repeated with new polymer–diluent samples. Again, three experiments were carried out at each experimental condition, and the droplet diameters measured as a function of time. Scaling exponents were determined to be 0.51 for the 10 wt%, 393 K condition and 0.45 for the 10 wt%, 388 K condition. These results are within the standard deviations of the earlier results.

When liquid–liquid TIPS experiments are carried out at a given temperature, and only the initial polymer concentration is changed, the only system property that changes is the droplet phase volume fraction, ν. As the initial polymer concentration decreases at a fixed temperature within the coexistence curve, the volume fraction of droplets increases as described above. The matrix phase viscosity and interfacial tension between the phases remain unchanged at a fixed temperatures*. Plotting the scaling exponents from *Table 7* against the volume fraction of droplets for all experimental conditions results in the plot shown in *Figure 10*.

At a fixed temperature the composition of the two phases formed upon phase separation is fixed irrespective of the initial polymer concentration. Therefore, γ_{12} and viscosity η remain constant irrespective of the initial polymer concentration. Thus, when the iPP–DPE samples of different initial polymer concentrations are phase separated at a fixed temperature the only parameter that is being varied is the volume fraction of the droplet phase. *Figure 10* shows a distinct increase in the

Table 7 Scaling exponents and standard deviations for kinetic experiments at all conditions, including standard deviations from the three experiments

Temperature (K)	Composition (iPP wt%)		
	10	15	20
398	0.36 ± 0.01		
393	0.47 ± 0.04	0.26 ± 0.01	0.22 ± 0.03
388	0.44 ± 0.03	0.32 ± 0.03	0.24 ± 0.03

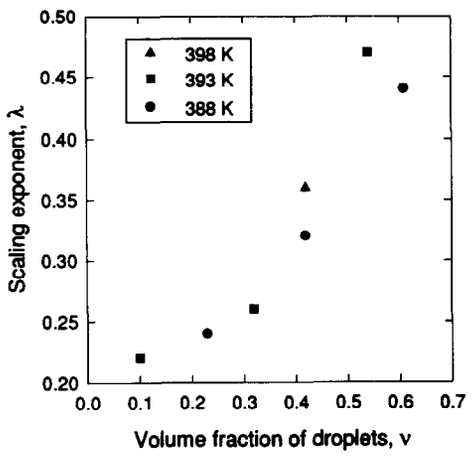

Figure 10 Dependence of scaling exponent, λ, on droplet phase volume fraction, ν

* These statements are only true if the cloud point curve is an accurate representation of the coexistence curve. It was shown in a previous publication[1] that for the iPP–DPE system used in this study this is indeed the case.

value of λ with increase in the volume fraction of the droplet phase.

Experimental data shown in *Figure 10* demonstrate that the droplet growth rates for the conditions 10 wt% at 398 K and 15 wt% at 388 K are almost identical. The volume fraction of the droplet phase at these two conditions are the same. The value of γ_{12}/η at 388 K and 398 K are 1.80×10^{-5} and 4.73×10^{-5} m s^{-1}, respectively. Thus the measured γ_{12}/η ratio is more than doubled. This indicates that the volume fraction of the droplet phase has a greater influence on the growth rate of the domains than the ratio of the interfacial tension between the phases to viscosity of the matrix phase.

CONCLUSIONS

The kinetics of droplet growth for a phase-separated system of poly(propylene) in diphenyl ether were measured under an optical microscope at three temperatures and three initial polymer concentrations. Droplet sizes ranged from 2 to 20 μm over time-scales of 700 s. It was found that the scaling exponent was highly dependent on the quench condition. A strong correlation between droplet phase volume fraction and scaling exponent was found which is not predicted by any existing theory. Scaling exponents ranged from 0.22 to 0.47 and droplet phase volume fractions ranged from 0.10 to 0.61. A new mathematical model will be published in a future paper that accounts for the deviation of the scaling exponents found in this work from existing theories.

ACKNOWLEDGEMENTS

The authors gratefully acknowledge the financial support of the Department of Defense and the Texas Advanced Technology Program.

REFERENCES

1 McGuire, K. S., Laxminarayan, A. and Lloyd, D. R. *Polymer* 1994, **35**, 4404
2 Caneba, G. T. and Soong, D. S. *Macromolecules* 1985, **18**, 2538
3 Tsai, F.-J. and Torkelson, J. M. *Macromolecules* 1990, **23**, 775
4 Vandeweerdt, P., Berghmans, H. and Tervoort, Y. *Macromolecules* 1991, **24**, 3547
5 Aubert, J. H. and Clough, R. L. *Polymer* 1985, **26**, 2047
6 Aubert, J. H. *Macromolecules* 1988, **21**, 3468
7 Aubert, J. H. and Sylwester, A. P. *Chemtech* 1991, **April**, 234
8 Callister, S., Keller, A. and Hikmet, R. M. *Makromol. Chem.: Macromol. Sym.* 1990, **39**, 19
9 Hikmet, R. M., Callister, S. and Keller, A. *Polymer* 1988, **29**, 1378
10 Song, S.-W. and Torkelson, J. M. *Macromolecules* 1994, **27**, 6389
11 Laxminarayan, A. *Thesis*, Michigan Technical University, 1990
12 Nojima, S., Tsutsumi, K. and Nose, T. *Polym. J.* 1982, **14**, 225
13 Lal, J. and Bansil, R. *Macromolecules* 1991, **24**, 290
14 Krishnamurthy, S. and Bansil, R. *Phys. Rev. Lett.* 1983, **50**, 2010
15 Nojima, S., Tsutsumi, K. and Nose, T. *Polym. J.* 1982, **14**, 289
16 Laxminarayan, A. *Dissertation*, The University of Texas at Austin, 1994, Ch. 1
17 Laxminarayan, A. *Dissertation*, The University of Texas at Austin, 1994, Ch. 4
18 Smolders, C. A., Aartsen, J. J. v. and Steenbergen, A. *Kolloid-Z. Z. Polym.* 1971, **243**, 14
19 Aubert, J. H. *Macromolecules* 1990, **23**, 1446
20 Shipman, G. H. US Patent 4 539 256, 1985
21 Vitzthum, G. H. and Davis, M. A. US Patent 4 490 431, 1984
22 Mrozinski, J. S. US Patent 4 726 989, 1988
23 Aggarwal, S. L. in 'Polymer Handbook' (Eds J. Bandrup, and E. H. Immergut) John Wiley, New York, 1975, p. 23
24 Kirshenbaum, I., Wilchinsky, Z. W. and Groten, B. *J. Appl. Polym. Sci.* 1964, **8**, 2723
25 Nakajima, A. and Saijyo A. *J. Polym. Sci.: Part A-2* 1968, **6**, 735
26 Laxminarayan, A., McGuire, K. S., Kim, S. S. and Lloyd, D. R. *Polymer* 1994, **35**, 3060
27 Laxminarayan, A. *Dissertation*, The University of Texas at Austin, 1994, Ch. 2
28 Van Krevelen, D. W. 'Properties of Polymers', 2nd Edn, Elsevier, Amsterdam, 1976
29 Cayias, J. L., Schechter, R. S. and Wade, W. H. in: 'Adsorption at Interfaces', (Ed. K. L. Mittal), ACS Symposium Series 8, Washington, DC, 1975
30 McGuire, K. S. *Dissertation*, The University of Texas at Austin, 1995, Ch. 3
31 Sanchez, I. C. 'Encylopedia of Physical Science and Technology', Vol. 12, Academic Press, New York 1992, p. 153
32 Gunton, J. D., Miguel, M. S. and Sahni, P. S. in 'Phase Transitions and Critical Phenomena', (Eds C. Domg and J. L. Lebowitz) Vol. 8, Academic Press, London, 1983
33 Kim, S. S. *Dissertation*, The University of Texas at Austin, 1990